

# Three-Dimensional Fluorophore Orientation Imaging with Multiview Polarized Microscopy

Talon Chandler,<sup>1,\*</sup> Min Guo,<sup>2</sup> Shalin Mehta,<sup>1,3,4</sup> Abhishek Kumar,<sup>2</sup>  
Hari Shroff,<sup>2,5</sup> Rudolf Oldenbourg,<sup>3,6</sup> Patrick J. La Rivière<sup>1,5</sup>

<sup>1</sup>Department of Radiology, University of Chicago, Chicago, Illinois 60637, USA.

<sup>2</sup>Section on High Resolution Optical Imaging, National Institute of Biomedical Imaging and Bioengineering, National Institutes of Health, Bethesda, Maryland 20892, USA.

<sup>3</sup>Bell Center, Marine Biological Laboratory, Woods Hole, Massachusetts 02543, USA.

<sup>4</sup>(present address) Chan Zuckerberg Biohub, San Francisco, California 94158, USA.

<sup>5</sup>Whitman Center, Marine Biological Laboratory, Woods Hole, Massachusetts 02543, USA.

<sup>6</sup>Department of Physics, Brown University, Providence, Rhode Island 02912, USA.

\*talochandler@talochandler.com

**Abstract:** We show that polarized fluorescence microscopes make band-limited measurements in the angular frequency domain. We use this result to propose and demonstrate efficient algorithms for reconstructing three-dimensional fluorophore orientations from multiview polarized microscope data.

**OCIS codes:** 180.2520 Fluorescence microscopy, 260.5430 Polarization

## 1. Introduction

Polarized fluorescence microscopes can measure the orientation of fluorophores in live specimens [1]. Unfortunately, existing techniques are limited to imaging two-dimensional orientations, and attempts to generalize these approaches to three-dimensional orientations have faced computational difficulties. We propose the use of the spherical harmonics to simplify the analysis of polarized fluorescence microscopes. In the same way that the Fourier transform simplifies the analysis of spatial imaging systems, the spherical Fourier transform simplifies the analysis of angular imaging systems.

## 2. Theory

Consider a small voxel that contains many non-interacting fluorophores. We define the orientation distribution function  $f(\hat{s})$  as the number of fluorophores per steradian oriented in a direction  $\hat{s}$ . The goal of polarized fluorescence microscopy is to estimate  $f(\hat{s})$  in many voxels throughout a three-dimensional sample.

The forward model for an  $N$ -measurement polarized fluorescence microscope is given by

$$g_i = \int_{\mathbb{S}^2} d\hat{s} h_i(\hat{s}) f(\hat{s}) \quad \text{for } i = 1, \dots, N, \quad (1)$$

where  $h_i(\hat{s})$  is the kernel of the  $i$ th microscope configuration, the integral is over the sphere  $\mathbb{S}^2$ , and  $g_i$  is the  $i$ th intensity measurement. Note that we are applying this forward model to each voxel independently—we assume that there is no spatial blurring so the signal from each voxel is independent. By discretizing  $f(\hat{s})$  and expanding  $h(\hat{s})$  in terms of the spherical harmonics, we can rewrite Eq. (1) as

$$\mathbf{g} = \Psi \mathbf{B}^+ \mathbf{f}, \quad (2)$$

where  $\mathbf{f} = [f(\hat{s}_1), \dots, f(\hat{s}_R)]^T$  is a vector of  $R$  samples of  $f(\hat{s})$ ;  $\mathbf{B}$  is a matrix of the spherical harmonics evaluated at the sample points,  $\mathbf{B}_{ij} = Y_j(\hat{s}_i)$  where  $Y_j$  is the  $j$ th spherical harmonic;  $\cdot^+$  is the Moore-Penrose pseudoinverse;  $\Psi$  is a matrix of the spherical harmonic coefficients of the kernels,  $\Psi_{ij} = \int_{\mathbb{S}^2} d\hat{s} h_i(\hat{s}) Y_j(\hat{s})$ ; and  $\mathbf{g} = [g_1, \dots, g_N]^T$  is a vector of the  $N$  intensity measurements.

The kernels for a wide class of polarized fluorescence microscopes have been calculated previously [2]. For many polarized fluorescence microscopes the kernel can be expanded in terms of a small number of spherical harmonics. If the kernel can be expanded in terms of  $M$  spherical harmonics then  $\Psi$  is an  $N \times M$  matrix and  $\mathbf{B}^+$  only needs to be calculated in the first  $M$  columns. This simplification reduces Eq. (1) from a set of integrals to an efficient series of matrix multiplications.

### 3. Methods and Results

We labeled the actin filaments of a fixed-cell sample with Alexa Fluor 488 Phalloidin and imaged the sample with an asymmetric 1.1/0.71 NA dual-view inverted selective plane illumination microscope with orthogonal objectives [3] and variable polarizers added to both illumination paths. The dipole moment of Alexa Fluor 488 Phalloidin is known to align parallel to the long axis of actin filaments, so this sample makes a suitable test specimen for our reconstruction algorithm. We imaged the specimen volume eight times—two views with four illumination polarization orientations each.

To reconstruct the orientation in each voxel we solved the following problem

$$\mathbf{f}^* = \underset{\mathbf{f} \in \{\mathbf{e}_i\} \ i=0,\dots,R}{\operatorname{argmin}} \quad \|\mathbf{g} - \Psi \mathbf{B}^+ \mathbf{f}\|_2^2, \quad (3)$$

where  $\mathbf{e}_i$  is a vector with a one in the  $i$ th entry and zeros elsewhere. By constraining  $\mathbf{f}$  we are assuming that all of the fluorophores in each voxel are oriented in the same direction—a reasonable assumption for this sample.

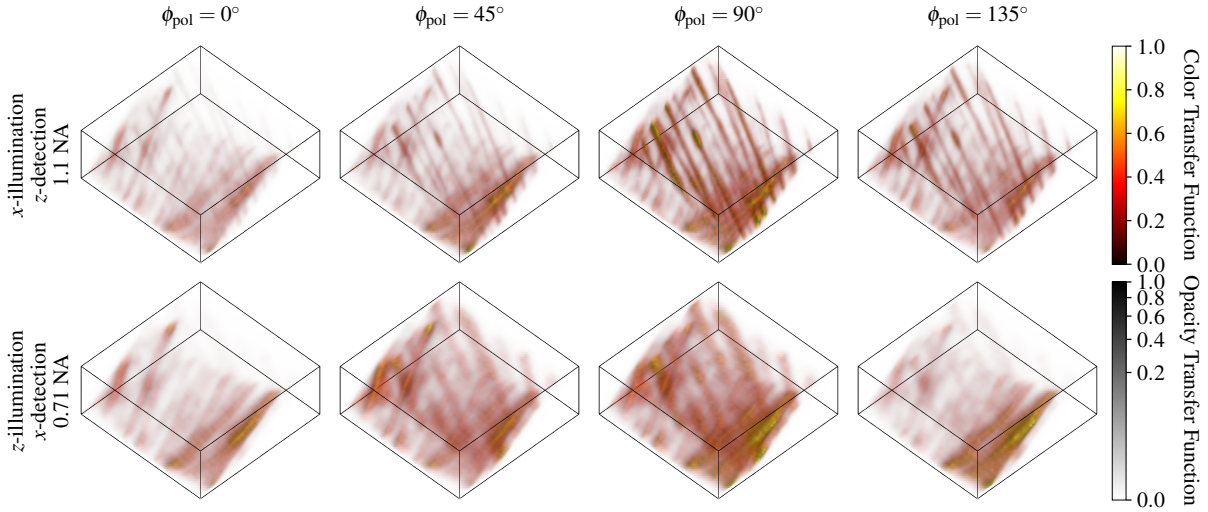


Fig. 1. Fluorescence intensities of a small volume ( $13.5 \times 13.5 \times 5.4 \mu\text{m}^3$ ) of a cell that was fixed, stained with Alexa Fluor 488 Phalloidin, and imaged in a dual-view microscope (diSPIM). The staining reveals two sets of actin bundles. Because fluorophores are aligned parallel to the bundles, their fluorescence intensities are modulated by the propagation direction and polarization of the excitation light. Bundles from bottom right to top left are highlighted for  $x$ -illumination and  $z$ -detection with  $\phi_{\text{pol}} = 90^\circ$ , while their intensities almost disappear for  $z$ -illumination and  $x$ -detection with  $\phi_{\text{pol}} = 0^\circ$ , which reveals the bundles running from bottom left to top right. The transfer functions at right use the normalized intensity value in each voxel to assign a color and opacity to each voxel.

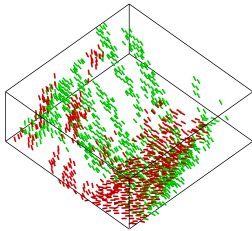


Fig. 2. Reconstruction of fluorophore orientations based on all intensity data shown in Fig. 1. Orientations are shown as short lines only in voxels whose fluorescence intensities surpassed a threshold. To highlight the two sets of actin bundles discussed in the caption of Fig. 1, we split the volume with a plane and colored the proximal voxels red and the distal voxels green. The reconstructed orientations approximately align with the long axes of the actin filaments as expected.

### References

1. S. Weiss, “Fluorescence spectroscopy of single biomolecules,” *Science* **283**, 1676–1683 (1999).
2. T. Chandler, S. Mehta, H. Shroff, R. Oldenbourg, and P. J. La Rivière, “Single-fluorophore orientation determination with multiview polarized illumination: modeling and microscope design,” *Opt. Express* **25**, 31,309–31,325 (2017).
3. Y. Wu, A. Kumar, C. Smith, E. Ardiel, P. Chandris, R. Christensen, I. Rey-Suarez, M. Guo, H. D. Vishwasrao, J. Chen, J. Tang, A. Upadhyaya, P. J. La Rivière, and H. Shroff, “Reflective imaging improves spatiotemporal resolution and collection efficiency in light sheet microscopy,” *Nat. Commun.* **8**, 1452 (2017).